The structural basis for an on–off switch controlling Gβγ-mediated inhibition of TRPM3 channels

Marc Behrendt[a,b,1,2], Fabian Gruss[c,1,3], Raissa Enzeroth[a,b], Sandeep Dembla[a,b], Siyuan Zhao[d], Pierre-Antoine Crassous[d], Florian Mohr[a], Mieke Nys[c], Nikolaos Louros[e], Rodrigo Gallardo[e,4], Valentina Zorzini[f,5], Doris Wagner[a], Anastassios Economou (Αναστάσιος Οικονόμου)[f], Frederic Rousseau[e], Joost Schymkowitz[e], Stephan E. Philipp[g], Tibor Rohacs[d], Chris Ulens[c,6], and Johannes Oberwinkler[a,b,6]

[a]Institut für Physiologie und Pathophysiologie, Philipps-Universität Marburg, 35037 Marburg, Germany; [b]Center for Mind, Brain and Behavior (CMBB), Philipps-Universität Marburg and Justus-Liebig-Universität Giessen, 35032 Marburg, Germany; [c]Laboratory of Structural Neurobiology, Department of Cellular and Molecular Medicine, KU Leuven, 3000 Leuven, Belgium; [d]Department of Pharmacology, Physiology and Neuroscience, Rutgers New Jersey Medical School, Newark, NJ 07103; [e]Switch Laboratory, VIB Center for Brain and Disease Research, Department of Cellular and Molecular Medicine, KU Leuven, 3000 Leuven, Belgium; [f]Laboratory of Molecular Bacteriology, Department of Microbiology and Immunology, Rega Institute for Medical Research, KU Leuven, 3000 Leuven, Belgium; and [g]Experimentelle und Klinische Pharmakologie und Toxikologie, Universität des Saarlandes, 66421 Homburg, Germany

Edited by László Csanády, Semmelweis University, Budapest, Hungary, and accepted by Editorial Board Member David E. Clapham August 27, 2020 (received for review February 13, 2020)

TRPM3 channels play important roles in the detection of noxious heat and in inflammatory thermal hyperalgesia. The activity of these ion channels in somatosensory neurons is tightly regulated by μ-opioid receptors through the signaling of Gβγ proteins, thereby reducing TRPM3-mediated pain. We show here that Gβγ directly binds to a domain of 10 amino acids in TRPM3 and solve a cocrystal structure of this domain together with Gβγ. Using these data and mutational analysis of full-length proteins, we pinpoint three amino acids in TRPM3 and their interacting partners in $Gβ_1$ that are individually necessary for TRPM3 inhibition by Gβγ. The 10-amino-acid Gβγ-interacting domain in TRPM3 is subject to alternative splicing. Its inclusion in or exclusion from TRPM3 channel proteins therefore provides a mechanism for switching on or off the inhibitory action that Gβγ proteins exert on TRPM3 channels.

GPCR signaling | TRP channels | alternative splicing | opioid analgesia

Nociceptive somatosensory neurons detect a large variety of events that signal real or potential danger of tissue damage, such as hot temperatures and noxious chemicals (1). The ensuing electrical signals, sent to the central nervous system, are therefore of immediate benefit for health and survival. Members of the large family of TRP proteins have emerged over the last two decades as important transducers of such danger signals in nociceptive neurons (2, 3). TRPM3 channels have recently been added to the list of pain-related TRP channels as important transducers of heat stimuli (4, 5) and as mediators in the development of inflammatory hyperalgesia (4, 6). TRPM3 proteins are expressed in dorsal root and trigeminal ganglia (4, 7–9) and form Ca^{2+}-permeable, nonselective cation channels (10–13) that can be activated, in addition to thermal stimuli, by the endogenous steroid pregnenolone sulfate (12), probably by direct interaction of the steroid with the channel proteins (14–16).

The sensitivity and response properties of nociceptive neurons are modulated by a large number of hormones and transmitters (17–19). A particularly striking example of such a modulation is the strong reduction of the electrical excitability due to endogenous or exogenous opioids (20), starting from the peripheral nerve endings of nociceptors (21) and continuing throughout the entire nociceptive system. Through this action, opioids are potent analgesic substances of immense clinical value for the management of diverse pain states. Clinically used opioids principally act via μ-opioid receptors (μORs), membrane-bound G protein-coupled receptors (GPCRs) coupled to $Gα_{i/o}$-containing heterotrimeric G proteins (22, 23). Activation of μORs leads to the release of Gβγ subunits that act on diverse targets in the plasma membrane, in particular on ion channels, to reduce nociceptive signaling (23). Recently, we and others have shown that TRPM3 channels are also subject to inhibition by activated μORs or other GPCRs (6, 24–28), a process that has been shown to take place in peripheral endings of nociceptive neurons since locally applied μOR or $GABA_B$ receptor agonists inhibit TRPM3-dependent pain (24–26).

Because pharmacotherapies with opioids have many and severe unwanted effects (29), there is intense interest in developing new and alternative analgesic substances, with down-stream effectors of μOR signaling being obvious candidates for new targets. Previously,

Significance

μ-Opioid receptors, activated by endogenous peptides or opioid drugs such as morphine, dampen the activity of nociceptor cells that detect noxious stimuli and thereby reduce pain. These receptors achieve this clinically important action by inhibitory signaling with Gβγ proteins to ion channels. Here we study how precisely Gβγ proteins inhibit one particular pain-related ion channel, TRPM3. Using TRPM3 splice variants, we identify a short stretch of amino acids required for the inhibitory action of Gβγ. We then characterize the interacting surfaces on both proteins by using X-ray crystallography. Our in-depth characterization of this protein–protein interaction can serve as a basis to facilitate the development of novel pain-reducing drugs impinging upon the specific interface between Gβγ and TRPM3.

Author contributions: M.B., F.G., S.D., S.Z., P.-A.C., F.M., N.L., R.G., V.Z., A.E., F.R., J.S., S.E.P., T.R., C.U., and J.O. designed research; M.B., F.G., R.E., S.D., S.Z., P.-A.C., F.M., N.L., R.G., V.Z., S.E.P., and J.O. performed research; M.B., F.G., R.E., M.N., and D.W. contributed new reagents/analytic tools; M.B., F.G., R.E., S.D., S.Z., P.-A.C., F.M., N.L., R.G., V.Z., A.E., F.R., J.S., S.E.P., T.R., C.U., and J.O. analyzed data; and M.B., F.G., A.E., F.R., J.S., S.E.P., T.R., C.U., and J.O. wrote the paper.

The authors declare no competing interest.

This article is a PNAS Direct Submission. L.C. is a guest editor invited by the Editorial Board.

[1]M.B. and F.G. contributed equally to this work.

[2]Present address: Experimental Pain Research, Heidelberg University, Medical Faculty Mannheim, 68167 Mannheim, Germany.

[3]Present address: Hubrecht Institute, Royal Netherlands Academy of Arts and Sciences, 3584 CT Utrecht, The Netherlands.

[4]Present address: Astbury Centre for Structural Molecular Biology, School of Molecular and Cellular Biology, University of Leeds, Leeds LS2 9JT, United Kingdom.

[5]Present address: Sir William Dunn School of Pathology, University of Oxford, Oxford OX1 3RE, United Kingdom.

[6]To whom correspondence may be addressed. Email: chris.ulens@kuleuven.be or johannes.oberwinkler@uni-marburg.de.

This article contains supporting information online at https://www.pnas.org/lookup/suppl/doi:10.1073/pnas.2001177117/-/DCSupplemental.

First published October 29, 2020.

therefore, the molecular details of the interaction of Gβγ proteins with their ion channel targets has been the subject of intensive investigation. This endeavor has been especially successful in defining the interactions between G protein-coupled inward rectifier K^+ (GIRK) channels and Gβγ proteins (30, 31). The inhibition of TRPM3 channels is also mediated by Gβγ subunits liberated after GPCR activation (6, 24–26). The molecular mechanisms of the TRPM3–Gβγ interaction are, however, so far unexplored. In this paper we show that Gβ proteins directly interact with TRPM3 and clarify the molecular details of this interaction by solving a cocrystal structure of a TRPM3 peptide bound to Gβγ protein.

Results

Gβγ subunits inhibit TRPM3 channels (24–28) by forming a multiprotein complex as demonstrated by coimmunoprecipitation experiments (24, 26). In order to gain insight into possible sites of interaction between Gβγ and TRPM3, we constructed a truncated version of the TRPM3 splice variant TRPM3α2, from which we removed the amino acids encoded by exons 1 to 3 and the complete C terminus downstream of amino acid 1330 (*SI Appendix*, Fig. S1*A*). When cotransfected with μORs, this artificial construct supported well-behaved pregnenolone sulfate–induced Ca^{2+} entry that was strongly inhibited by activation of the μORs (*SI Appendix*, Fig. S1 *B* and *C*), indicating that neither the extreme N nor much of the C terminus of TRPM3 is required for GPCR-mediated inhibition. These data led us to hypothesize that the interaction between TRPM3 and Gβγ proteins takes place principally on the cytosolic N-terminal region of TRPM3, but not on the amino acids encoded by the first three exons.

Exon 17 of TRPM3 Is Necessary for the Inhibition of TRPM3 by Gβγ. The N-terminal region of TRPM3 is subject to alternative splicing at least at four different sites (11, 32–34). We therefore wondered whether any of these splice events might interfere with the inhibitory coupling of Gβγ to TRPM3. We expressed a panel of previously described splice variants (11, 33) together with μORs in HEK293 cells. Using Ca^{2+} imaging (Fig. 1*A* and *SI Appendix*, Fig. S2*A*) or whole-cell patch-clamp electrophysiology (Fig. 1*B* and *SI Appendix*, Fig. S2 *C–H*), we found that all splice variants, but not TRPM3α4 and TRPM3α5, were inhibited upon activation of μORs. Furthermore, when we severely truncated TRPM3α5 by again removing the amino acids encoded by exons 1 to 3 and most of the C-terminal amino acids (*SI Appendix*, Fig. S1*A*), we found that the inhibition caused by GPCR activation was still completely absent, similar to the results obtained with full-length TRPM3α5 (*SI Appendix*, Fig. S1 *B* and *C*). In essence, the truncated TRPM3 mutants constructed from TRPM3α2 and TRPM3α5 behaved like their full-length counterparts (Fig. 1 *A* and *B* and *SI Appendix*, Fig. S1).

Since previous publications strongly indicated that GPCR activation inhibits TRPM3 channels by liberating Gβγ subunits (24–26) we next investigated whether the various splice variants were differentially sensitive to Gβγ overexpression. In complete agreement with the experiments above, we found that the activity of all splice variants, with the exception of TRPM3α4 and TRPM3α5, was strongly reduced by overexpressing $Gβ_1γ_2$, (Fig. 1*C* and *SI Appendix*, Fig. S2*B*). TRPM3α4 and TRPM3α5 share a splice event, the removal of exon 17, but in all other measured splice variants exon 17 is retained. Furthermore, the other N-terminal splice events (at exons 8 and 15) do not segregate with the observed sensitivity to Gβγ [Fig. 1*D*; the splice event at exon 13 could not be investigated since variants without exon 13 do not form functional ion channels (33)]. Exon 17 is short, encoding for 10 amino acids, which are not found in other TRPM channels, except in TRPM1, the protein most closely related to TRPM3. These data indicate that the 10 amino acids encoded by exon 17 are essential for the functional inhibition caused by Gβγ on TRPM3 channels.

The TRPM3 Exon 17–Encoded Peptide Interacts with Gβγ. The amino acids encoded by exon 17 are required for the functional inhibition of TRPM3 channels by Gβγ, but this does not necessarily imply that Gβγ binds directly to these amino acids. We tested therefore whether a short peptide, representing the exon 17–encoded amino acids, binds to Gβγ proteins. By coupling the 10 amino acids encoded by exon 17 to a His-tagged maltose-binding protein (*SI Appendix*, Fig. S3*A*), we were able to immobilize this peptide on a nickel column. Note that the sequence of the peptide was extended by two N-terminal and three C-terminal surrounding amino acids yielding the final sequence: K_{592}RPKALKLLGMEDDI$_{606}$ (exon 17–encoded residues are underlined, and subscripted numbering indicates the amino acid position in full-length TRPM3α2). Applying solutions to this column containing purified $Gβ_1γ_2$ [not containing a His-tag and made water-soluble by a C68S mutation in $Gγ_2$ (35)], we found that Gβγ was partly retained by the exon 17–encoded peptide (*SI Appendix*, Fig. S3 *B* and *C*). To test the specificity of this retention, we cleaved off the exon 17–encoded peptide from the maltose-binding protein with thrombin, which significantly reduced the retention of Gβγ, thus showing that Gβγ was indeed interacting with the exon 17–encoded peptide (*SI Appendix*, Fig. S3 *B* and *C*).

We next immobilized an N-terminally biotinylated version of the exon 17–encoded peptide (biotin-Ahx-K_{592}RPKALKLLGMEDDI$_{606}$; exon 17–encoded residues underlined) onto streptavidin-coated biosensors for bio-layer interferometry (BLI) binding experiments. Dipping the sensors with the bound peptides into solutions containing increasing concentrations of water-soluble Gβγ, we measured the binding of Gβγ to the sensor. The equilibrium responses showed a saturating behavior that was well fitted by assuming a 1:1 binding model with an apparent binding constant $K_d = 55.9 \pm 12.9$ μM ($n = 3$, *SI Appendix*, Fig. S3 *D* and *E*). While this value seems to indicate a low affinity between the TRPM3 peptide and Gβγ, in living cells both proteins, TRPM3 and Gβγ, are located in or tethered to the plasma membrane, thereby increasing their local concentrations as well as limiting the space for diffusion and thus vastly increasing the chances of molecular encounters.

To further demonstrate the specificity of the interaction, we conducted competitive binding experiments using the same experimental design and fixed concentrations of water-soluble Gβγ (either 4.9 or 19.3 μM) and added nonbiotinylated (and therefore not immobilized) peptide at increasing concentrations. The responses at both Gβγ concentrations clearly showed a decrease of the signal with increasing free peptide concentration (*SI Appendix*, Fig. S3 *F–I*), indicating that the free peptide competes with the immobilized peptide for binding to a specific site of Gβγ. When we repeated these experiments by adding a peptide mutated at four amino acid positions compared to the original peptide, we found that this mutated peptide was unable to compete with the original peptide for binding to Gβγ (*SI Appendix*, Fig. S3 *J* and *K*), further confirming the specificity of this interaction. Taken together, these experiments clearly establish that a short peptide encoded by exon 17 of TRPM3 has the capacity to bind to Gβγ.

The Region of TRPM3 Encoded by Exon 17 Might Be the Principal Binding Site of Gβγ. Having established that the part of the TRPM3 protein encoded by exon 17 is both necessary for the Gβγ-mediated inhibition of TRPM3 (Fig. 1) and capable to bind Gβγ (*SI Appendix*, Fig. S3), we wondered whether any other part of the fairly large TRPM3 proteins is capable of binding Gβγ. We therefore analyzed the TRPM3–Gβγ interaction systematically by dot blot analysis of the complete TRPM3 protein sequence (*SI Appendix*, Fig. S4). The TRPM3α2 sequence of 1,709 residues was sequentially scanned using consecutive 25-mer polypeptides overlapping the preceding peptide by 21 residues each (36). Gβγ proteins bound strongly to two groups of consecutive polypeptides (*SI Appendix*, Fig. S4*A*; peptides 17 to 21 and peptides 144 to 147). The peptides with

apparent Gβγ binding in the two groups have the common sequences P_{81}STKDPHRC$_{89}$ and Y_{585}HNLFGPKRPKAL$_{597}$, respectively. We designated these regions putative binding regions 1 and 2 and analyzed them in more detail. Starting with amino acid residue P_{81} and ending with R_{93}, successive replacement of amino terminal residues by alanine reduced the binding of Gβγ to binding site 1 stepwise from 95 to 2% (*SI Appendix*, Fig. S4*B*, *Right*). Correspondingly, replacement of C-terminal amino acid residues R_{93} to K_{84} diminished Gβγ interaction completely (*SI Appendix*, Fig. S4*B*, *Left*). However, replacement of single amino acid residues by

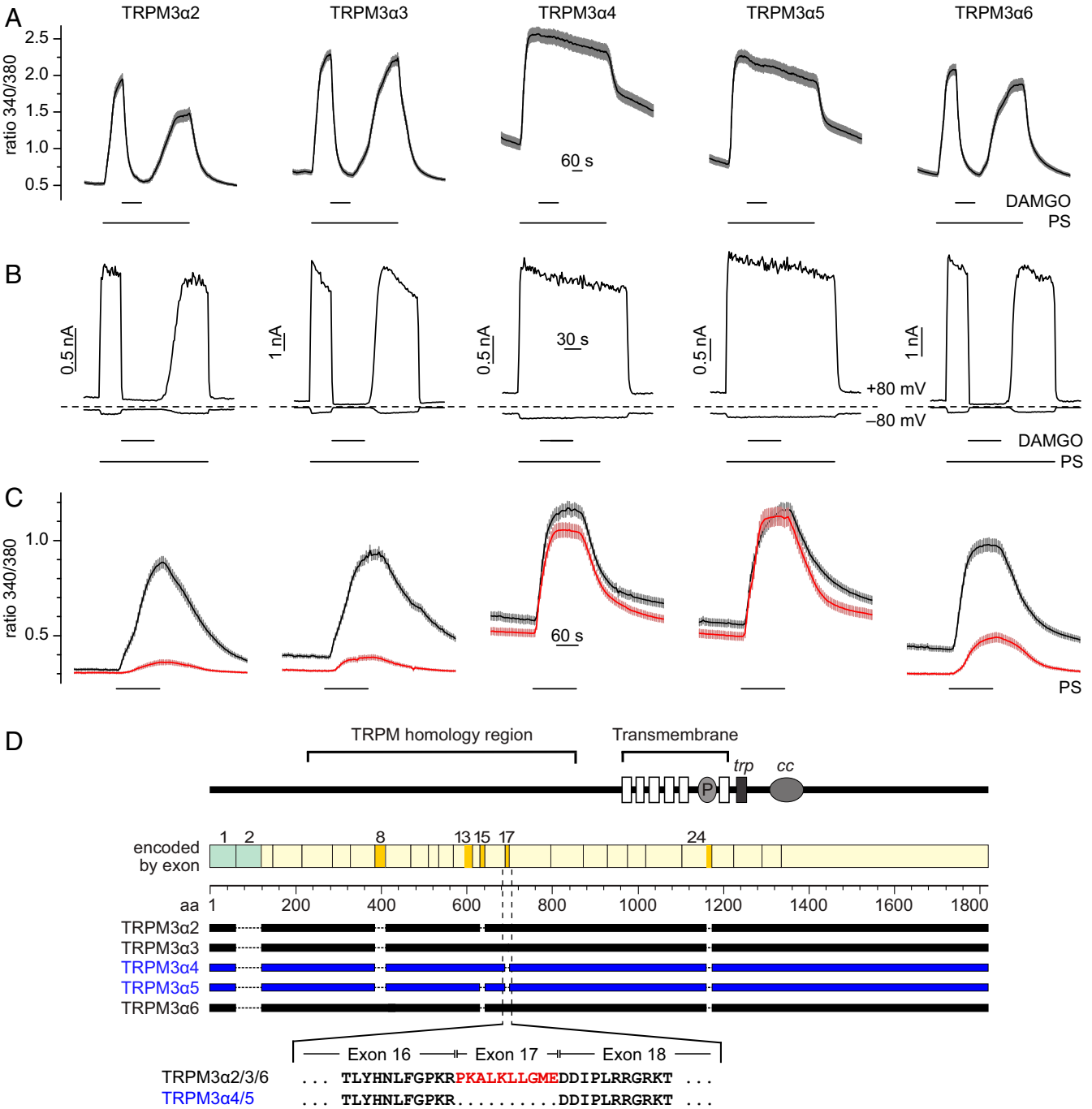

Fig. 1. TRPM3 splice variants are differentially susceptible to inhibition by Gβγ. (*A*) Fura-2 imaging experiments with HEK293 cells cotransfected with the splice variant indicated and μORs show that pregnenolone sulfate (PS)-activated (50 μM PS) TRPM3α4 and TRPM3α5 are not inhibited by μOR activation (3 μM DAMGO), while the other splice variants are profoundly inhibited. (*B*) Cells similarly transfected were assayed in whole-cell patch-clamp experiments. Each panel depicts a recording of a single representative cell. (*C*) Fura-2 experiments with cells transfected with Gβγ and a splice variant of TRPM3 (red traces). Black traces show control experiments, in which Gβγ was not transfected. The statistical analysis of the data shown in *A*–*C* is given in *SI Appendix*, Fig. S2. (*D*) Schematic drawing outlining the different splicing events giving rise to the five splice variants investigated (adapted from ref. 33). In the lower half, the amino acid sequences at the junctions of exons 16 and 17 and 17 and 18 are depicted, and amino acids encoded by exon 17 are shown in red. These amino acids are lacking in the splice variants TRPM3α4 and TRPM3α5.

alanine only slightly affected the binding of Gβγ (*SI Appendix*, Fig. S4*C*). There are, however, two reasons why it is unlikely that Gβγ mediates its inhibitory effect on TRPM3 channels via binding to this putative binding region 1. First, truncating the N terminus in a way that impacts this putative binding site did not alter the Gβγ-mediated inhibition of TRPM3 channels (*SI Appendix*, Fig. S1). Second, the location in the very N terminus is unlikely to allow for binding to membrane-bound Gβγ (*Discussion*). We therefore focused next on putative binding site 2, which we analyzed in a similar manner (*SI Appendix*, Fig. S4 *D* and *E*). In contrast to binding site 1, we found for the second binding site that single lysine residues play a prominent role for the interaction with Gβγ proteins. Replacement of K_{592}, K_{595}, and K_{598} displayed a pronounced reduction of signal intensity after successive (*SI Appendix*, Fig. S4*D*) as well as after single replacement of residues by alanine (*SI Appendix*, Fig. S4*E*). Furthermore, the exchange of a number of additional residues affected the binding of Gβγ. Importantly, binding site 2 encompasses four amino acids that are encoded by exon 17. Thus, the dot blot analysis provides additional support for the identification of the protein region encoded by exon 17 as a candidate for the interaction site of TRPM3 and Gβγ.

Exon 17–Encoded Amino Acids Are Involved in Gβγ Binding to TRPM3. If the region encoded by exon 17 is indeed a main site where Gβγ proteins interact with TRPM3, as indicated by the dot blot analysis, binding of Gβγ to full-length TRPM3 splice variants without exon 17 should be reduced. We tested this by coimmunoprecipitation experiments and directly compared the splice variants TRPM3α2 (with exon 17–encoded amino acids) and TRPM3α5 (without these amino acids). In all five experiments we detected more Gβ proteins coprecipitating with TRPM3α2 than with TRPM3α5, indicating that Gβ proteins indeed bind better to TRPM3α2 compared to TRPM3α5 (*SI Appendix*, Fig. S5 *A*–*C*). However, we also noticed that we consistently precipitated more TRPM3α5 than TRPM3α2 (*SI Appendix*, Fig. S5*A*). Attempting to correct for the different amount of TRPM3 proteins pulled down enlarged the difference in Gβ binding between the two splice variants (*SI Appendix*, Fig. S5 *D* and *E*). These data are thus compatible with the idea that Gβγ proteins bind to exon 17–encoded amino acids of full-length TRPM3 proteins.

Single-Point Mutations in TRPM3 Exon 17 Strongly Reduce GPCR-Induced Channel Inhibition. The dot blot analysis of the region in and around exon 17 indicated that Gβγ binding to TRPM3 could be sensitive to single amino acid substitutions (*SI Appendix*, Fig. S4*E*). We wanted to test this hypothesis for full-length TRPM3 proteins and therefore mutated each of the 10 amino acids encoded by exon 17. Coexpressing these mutant TRPM3 proteins with μORs and monitoring the intracellular Ca^{2+} concentration, we investigated whether TRPM3 inhibition caused by μOR stimulation was altered (Fig. 2). This assay also ascertained that all channel proteins carrying a single-point mutation were still functional, as they all produced pregnenolone sulfate–induced Ca^{2+} signals. The results showed clearly that specific single-point mutations indeed severely reduce or abolish GPCR-induced TRPM3 inhibition. In particular, we found that mutation of the lysine at position 595 of full-length TRPM3α2 (K_{595}, equivalent to position 2 of exon 17), of two leucines (L_{599} and L_{600}), and of the glycine (G_{601}) severely compromised μOR activation-induced TRPM3 inhibition (Fig. 2*A* and *SI Appendix*, Fig. S6*A*). In the case of K_{595}, we also tested the effects of mutating this residue to other amino acids. Mutating K_{595} to histidine or even reversing its charge by mutating to aspartate, the resulting (still functional) channels were again not inhibited by μOR activation (Fig. 2*B* and *SI Appendix*, Fig. S6 *B* and *C*). Similarly, we tested the consequences of mutating the alanine at position 3 of exon 17 (A_{596}) to glycine, a mutation that we previously had investigated in the dot blot analysis (*SI Appendix*, Fig. S4*E*). This mutation had a considerably stronger effect on TRPM3 inhibition than the A_{596}-to-histidine mutation (*SI Appendix*, Fig. S6 *B* and *C*). Finally, we mutated the three amino acids preceding exon 17 to alanine, but those mutations did not impede receptor-induced inhibition (*SI Appendix*, Fig. S6 *D* and *E*). Together, these data indicate that some, but not all, amino acids of TRPM3 exon 17 individually play a decisive role in the inhibition of TRPM3 channels by GPCR activation. Of special importance appear to be K_{595}, L_{599}, L_{600}, and G_{601} (Fig. 2*B*). Notably, K_{595} already proved important in the dot blot analysis (*SI Appendix*, Fig. S4 *D* and *E*).

Crystal Structure of Gβγ in Complex with TRPM3 Exon 17–Encoded Peptide. To understand at atomic resolution how these specific amino acids interact with $Gβ_1γ_2$, and why their substitutions are detrimental to this interaction, we cocrystallized the 15-amino-acids-long, nonbiotinylated peptide (identical to the one used in the competitive binding studies of *SI Appendix*, Fig. S3 *F*–*I*) with $Gβ_1γ_2$ and used the collected X-ray diffraction data to determine the structure (resolution: 1.94 Å; for data collection and refinement statistics see *SI Appendix*, Table S1). We used the electron density map to build residues 4 to 340 of $Gβ_1$, 7 to 68 of $Gγ_2$, and 13 out of 15 amino acids of the peptide (Fig. 3*A*). $Gβ_1$ shows the known β-propeller fold composed of seven WD40-repeat blades, and also the $Gβ_1$-bound $Gγ_2$ adopted its well-known conformation (37–39). The TRPM3 peptide forms extensive interactions with $Gβ_1$ but not with the spatially distant $Gγ_2$. Residues R_{593} to L_{600} of the peptide adopt an α-helical structure and are located on top of $Gβ_1$, close to the central axis of the β-propeller. Peptide residue G_{601} breaks the α-helical fold by introducing a sharp kink, from which the rest of the peptide protrudes away from Gβ (Fig. 3*B*). We wondered whether the α-helical fold of the peptide observed in the crystal structure is induced by the binding to $Gβ_1γ_2$, or whether the peptide is intrinsically α-helical. Circular dichroism spectroscopy measurements of the free peptide in solution showed a signal typical for a random coil structure, while the predicted signal calculated from the peptide bound to Gβ displayed the well-established spectrum of α-helical peptides (Fig. 3*C*). We conclude, therefore, that the α-helical fold of the TRPM3-encoded peptide in the crystal structure is specific for the $Gβ_1$-bound state only.

Between $Gβ_1$ and the TRPM3 peptide several electrostatic, polar, and hydrophobic interactions can be observed in the structure (Fig. 3*B*). The positively charged amino group of the side chain of peptide residue K_{595} forms electrostatic and polar interactions with the side chains of D228, N230, and D246 of $Gβ_1$. A hydrogen bond is formed between the carbonyl oxygen of peptide L_{600} and the hydroxyl group of $Gβ_1$ Y59. Water-mediated contacts are formed between the carbonyl group of peptide L_{599} and the nitrogen in the side chain of W332 of $Gβ_1$. Furthermore, TRPM3 peptide residues A_{596}, L_{599}, and L_{600} are part of a hydrophobic interaction interface formed with $Gβ_1$ residues Y59, W99, M101, L117, Y145, M188, and W332. The charged and uncharged areas in the surfaces of the binding sites of $Gβ_1$ and the TRPM3 peptide are distributed in a way that they complement each other upon binding (Fig. 3*D*). In summary, the exon 17–encoded residues of the peptide that are directly involved in interactions with $Gβ_1$ in the structure are K_{595}, A_{596}, L_{599}, and L_{600}. This information learned from the three-dimensional (3D) structure can be compared to the mutagenesis data of the full-length TRPM3α2 channels (Fig. 2): K_{595}, L_{599}, and L_{600} are critically important for the functional interaction of TRPM3 channels and Gβγ, in full agreement with their interacting pose in the 3D crystal structure. Changing A_{596} to histidine was tolerated for the functional interaction, while a change to glycine was not, possibly indicating that the flexible glycine disrupts the α-helical conformation. M_{602} appears to interact to a lesser degree with Gβ and an alanine can apparently be substituted

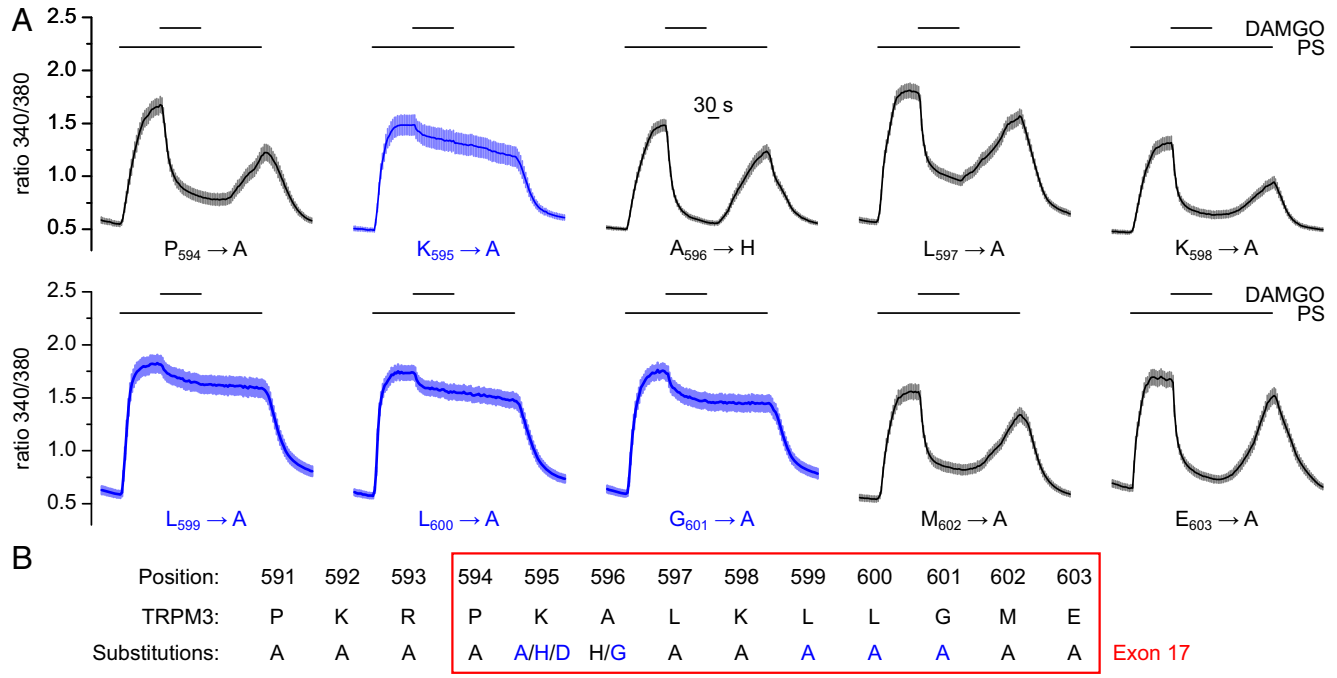

Fig. 2. Individual amino acids encoded by exon 17 are crucial for the GPCR-mediated inhibition of TRPM3 channels. (*A*) The 10 amino acids encoded by exon 17 were individually mutated (to alanine or histidine, as indicated). After coexpression in HEK293 cells with μORs, the inhibition induced by activation of μORs (3 μM DAMGO) of the pregnenolone sulfate (PS)-induced Ca^{2+} signals (50 μM PS) was measured. Of the mutants investigated, K_{595}A, L_{599}A, L_{600}A, and G_{601}A showed the strongest defects in the μOR-mediated inhibition. The single-cell analysis of these data is given in *SI Appendix*, Fig. S6*A*. Results from further mutations of amino acids in and in the vicinity of exon 17 are reported in *SI Appendix*, Fig. S6 *B–E*. (*B*) Summary of the mutations analyzed in *A* and in *SI Appendix*, Fig. S6. Blue indicates that the mutation strongly reduced or abolished TRPM3 channel inhibition due to μOR activation.

without functional impairment. We conclude that the findings from the 3D structure agree very well with the mutagenesis data and rationalize them to a large degree.

Mutagenesis of $G\beta_1$ Confirms the Functional Importance of Its Interactions with TRPM3 Exon 17. The 3D crystal structure also permits identification of the amino acid residues of the $G\beta_1$ protein that interact with the exon 17–encoded peptide. In particular, as mentioned above, the $G\beta_1$ residues Y59, W99, M101, L117, Y145, M188, D228, N230, D246, and W332 directly contribute to interactions with the exon 17–encoded residues of the peptide. To examine the roles of these and additional $G\beta_1$ residues in TRPM3 inhibition, we first took an unbiased approach and tested $G\beta_1$ mutants described earlier to alter activation or inhibition of various downstream effectors of Gβγ, such as GIRK channels and N-type voltage-gated Ca^{2+} channels (30). As the mutants of $G\beta_1$ described by Ford et al. (30) are surface-accessible and were all tested for proper folding and surface expression, we measured pregnenolone sulfate–induced currents (see representative traces in Fig. 4*A*) after coexpressing the mutant $G\beta_1$ proteins together with $G\gamma_2$ and hTRPM3 in *Xenopus laevis* oocytes (24). First, we tested alanine mutations of four residues (L55, K78, K89, and W99) that were shown to alter GIRK channel activation (30) and were later shown to be in close contact with the channel in the GIRK–Gβγ cocrystal structure (31). The W99A mutant of $G\beta_1$ showed no inhibition of TRPM3, but the remaining three mutants (L55A, K78A, and K89A) showed robust inhibition of TRPM3 currents, similar to that induced by the wild-type $G\beta_1$ (Fig. 4*B* and *SI Appendix*, Fig. S7*A*), indicating that the residues interacting with GIRK are different from those responsible for TRPM3 inhibition, with some overlap. In three additional rounds of experiments, we tested another 11 $G\beta_1$ mutants and found that $G\beta_1$ mutants I80A, L117A, M101A, and D228A induced no significant inhibition of TRPM3. The mutants K57A, Y59A, and W332A showed some inhibition, but it was significantly lower than that induced by wild-type $G\beta_1$ (Fig. 4*B* and *SI Appendix*, Fig. S7*A*). The rest of the mutants (S98T, N119A, T143A, and D186A) showed inhibition similar to wild-type Gβγ.

Overall, mutating $G\beta_1$ residues that are in direct contact with the TRPM3 peptide (Y59, W99, M101, L117, D228, and W332), or located close (K57 at a distance of approximately 4.5 Å), either significantly reduced or eliminated TRPM3 inhibition (Fig. 4*D*). Conversely, mutation of $G\beta_1$ residues that are located far away from the peptide (L55, K78, K89, S98, N119, and T143) had no effect on Gβγ inhibition, with one exception (I80A). Whether the I80A mutation exerted an indirect effect through changing the conformation of Gβγ or it is in contact with other parts of the full-length channel is not clear. On the other hand, D186 of $G\beta_1$ appears close to the exon 17–encoded peptide in the structure, but its mutation (D186A in Fig. 4*B*) did not have a statistically significant effect on Gβγ-mediated inhibition of TRPM3. This, however, is perhaps not surprising considering that D186 forms a strong H-bond with the first K residue (K_{592}) of the TRPM3 peptide through its N-terminal primary amine. In the full-length channel this primary amino group is involved in a peptide bond and the N-H is probably less available for H-bonding, potentially rationalizing the lack of a significant effect of the D186A mutation.

Guided by the crystal structure, we also analyzed in more depth the interaction of K_{595} with $G\beta_1$, this time employing overexpression of $G\beta_1$ mutants, $G\gamma_2$, and TRPM3α2 in HEK293 cells with subsequent Ca^{2+} imaging. In this series of experiments, we used Myc-tagged $G\beta_1$ proteins, in order to be able to detect their expression levels over the background of the Gβ proteins endogenously expressed by the HEK293 cells. The positively charged exon 17 residue K_{595} interacts with at least three negatively charged amino acids of $G\beta_1$ (D228, N230, and D246; Fig. 3*B*). Overexpression of the $G\beta_1$ mutants D228A, D228R, N230A, and D246S [D246 was mutated to serine, because it has

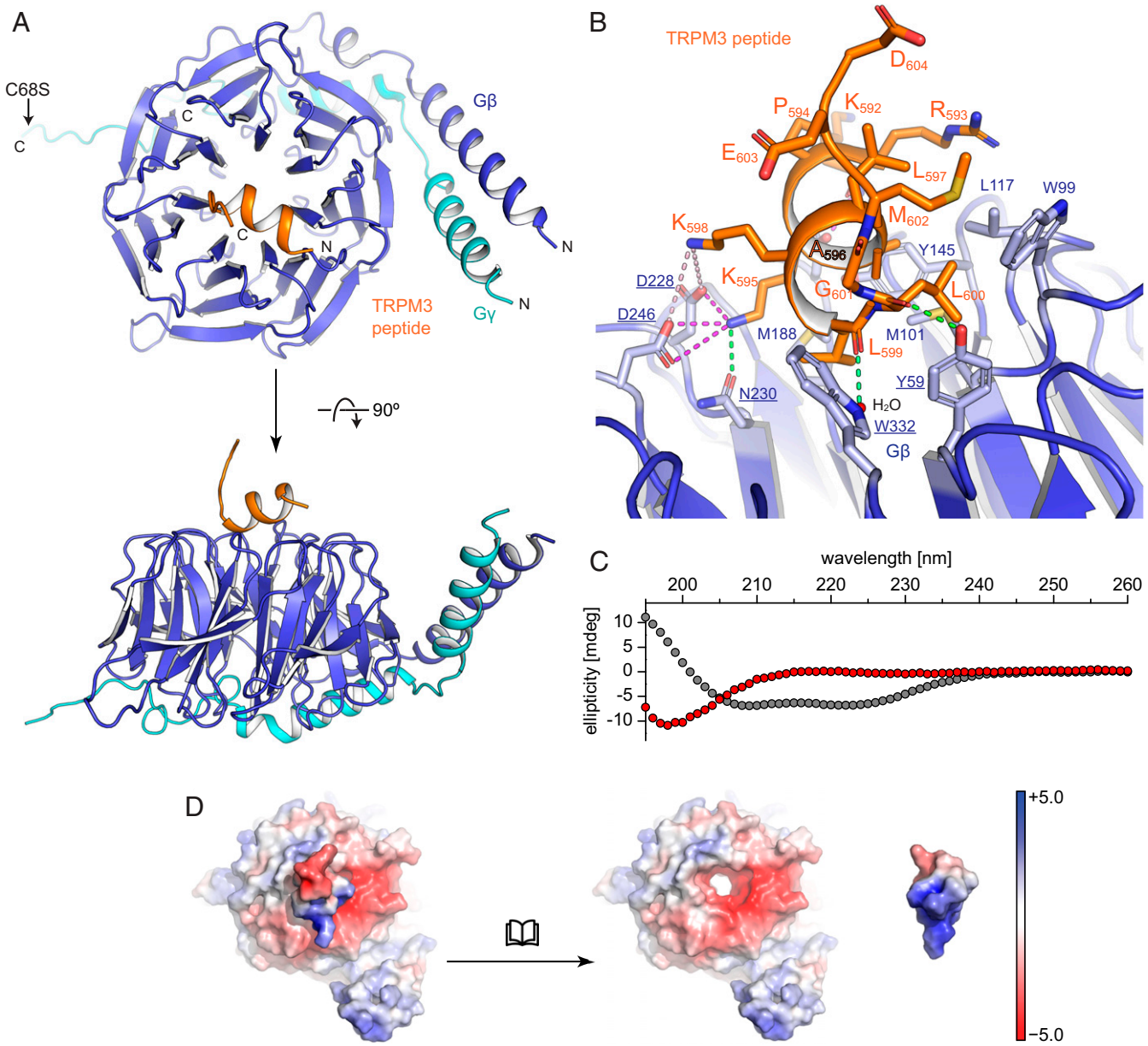

Fig. 3. Structural analysis of the TRPM3 peptide bound to Gβγ. (*A*) Overview of the cocrystal structure of Gβγ and a peptide encompassing the TRPM3 exon 17–encoded amino acids in backbone representation with Gβ in blue, Gγ in cyan, and the TRPM3 peptide in orange. (*B*) A zoom-in to the interaction interface is shown in cartoon and stick representation. For Gβ (blue) only side chains involved in interactions are shown (labeled in blue and underlined for residues undergoing polar interactions and blue and not underlined for residues involved in hydrophobic interactions); for the peptide (orange) all side chains are shown. Polar interactions are indicated with dotted lines for electrostatic interactions (magenta for salt bridges and light magenta for long-range interactions) and hydrogen bonds (green). (*C*) Secondary structure analysis (using circular dichroism spectroscopy) of the peptide in solution (red dots, alone without interaction partners) shows the signal of a random coil structure. The calculated circular dichroism spectrum of the bound peptide (gray dots) has been included to demonstrate the signal expected from an α-helix. (*D*) Visualization of surface charges (calculated as "charge-smoothed potential" in PyMOL; red colors indicate negative charges, blue colors positive charges) of the TRPM3 peptide bound to Gβγ (*Left*) and of both parts displayed separately (*Right*) demonstrating the complimentary charges on the interacting surfaces. Note that the TRPM3-encoded peptide has been turned by 180° to reveal the charges on the surface that touches Gβ.

previously been reported that the D246A mutant is unstable (39)] resulted in pregnenolone sulfate–induced activity of TRPM3 (as judged from the increase in intracellular Ca^{2+}) that was equally or less inhibited compared to the overexpression of wild-type $Gβ_1$ (Fig. 4*C* and *SI Appendix*, Fig. S7*B*). When we analyzed the relative expression levels, however, we found that the mutants were expressed at lower levels compared to the wild-type $Gβ_1$ protein, complicating the interpretation of the results (*SI Appendix*, Fig. S7*C*). The overexpression of $Gβ_1$ mutants D228R and N230A did not induce any inhibition of TRPM3 channel activity (Fig. 4*C*), despite clear, albeit reduced, expression of these mutants (*SI Appendix*, Fig. S7*C*). The results obtained with these two mutants therefore establish that the interaction partners of K_{595} play an important role in the functional consequences of Gβγ binding to TRPM3. They thereby corroborate our earlier findings with the D228A mutant in the oocyte system (Fig. 4*B*). We equally overexpressed the Myc-$Gβ_1$ Y145A mutant, as this residue participates in the hydrophobic interactions of TRPM3 exon 17–encoded L_{599}

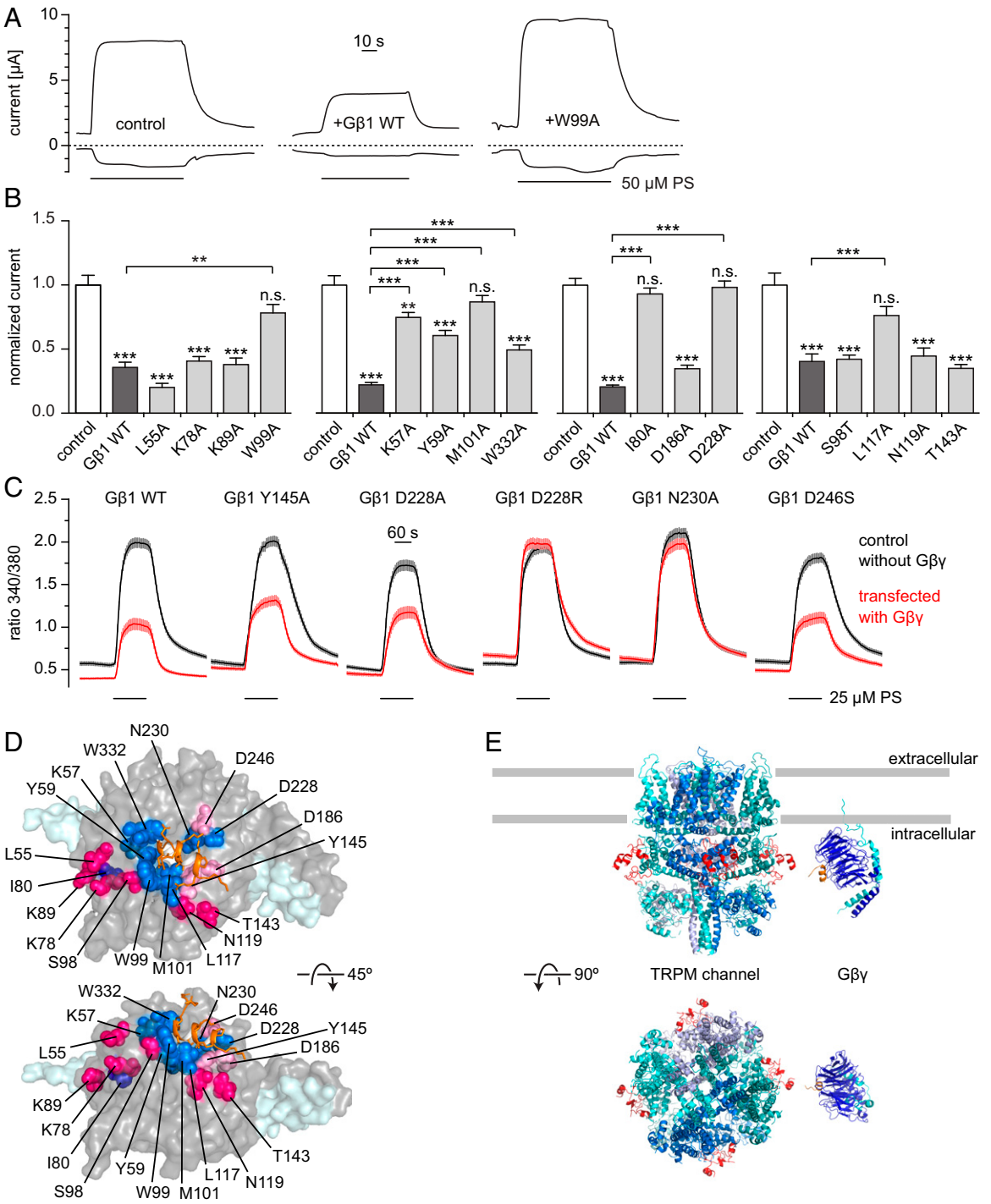

Fig. 4. Effects of Gβ mutations on the inhibition of TRPM3. (*A*) Representative current traces (at −100 and +100 mV) of two-electrode voltage clamp experiments performed in *Xenopus* oocytes expressing hTRPM3, $G\gamma_2$ and wild-type or mutated $G\beta_1$; 50 µM pregnenolone sulfate (PS) was applied as indicated, dashed lines denote zero current. (*B*) Summary data showing current amplitudes normalized to the average current induced by 50 µM PS in control oocytes without Gβγ coexpression in the same experiment. Mutants tested in the same experiments were grouped into the same panel. Asterisks above columns indicate significant difference from control oocytes without Gβγ expression (*$P < 0.05$; **$P < 0.01$; ***$P < 0.001$; n.s., $P \geq 0.05$). (*C*) Ca^{2+} imaging experiments in TRPM3-expressing HEK293 cells transiently transfected with $G\gamma_2$-IRES-GFP and Myc-tagged $G\beta_1$ (wild-type or mutant, red) or empty vectors as controls (black). When using the mutants D228R and N230A, the strong reduction in PS-induced Ca^{2+} signals seen with wild-type Gβ was not observed. *SI Appendix*, Fig. S7 shows single cell responses for the data in *A*–*C*, as well as expression controls for mutant $G\beta_1$ proteins. (*D*) Visual summary of the Gβ mutagenesis experiments. Residues that reduced or abolished the inhibition of TRPM3 when mutated are shown as blue spheres, the TRPM3-encoded peptide is drawn as orange sticks. Residues not having an effect on TRPM3 inhibition when mutated are shown as red or pink spheres depending on the apparent distance to the TRPM3 peptide. (*E*) Cartoon of the proposed model: Gβγ binds to the linker region between MHR3 and MHR4 (red) located on the outer surface of the channel and at a suitable distance from the plasma membrane for binding to membrane-bound Gβγ. Since a 3D structure for TRPM3 is not available, the closely related TRPM7 [PDB ID code 6BWF (49)] is depicted (see *SI Appendix*, Fig. S8C for additional TRPM structures). The Gβγ structure (blue and cyan) with the TRPM3-encoded peptide (orange) is the 3D structure described in this paper. Gray bars approximately indicate the plasma membrane boundaries.

and L_{600} with $G\beta_1$ (Fig. 3*B*). While we observed a reduced TRPM3 inhibition when we overexpressed this mutant, we also found that this mutant Gβ protein only expressed weakly in HEK293 cells (Fig. 4*C* and *SI Appendix*, Fig. S7*C*). Therefore, we could not draw any firm conclusion about the involvement of Y145 in the interaction of TRPM3 and $G\beta_1$.

Taken together, single mutations of $G\beta_1$ residues that were in close contact with the TRPM3 exon 17–encoded peptide reduced or eliminated TRPM3 inhibition (Fig. 4 *B*–*D*). Mutations of residues located at a greater distance had (with one exception) no effect on channel inhibition (Fig. 4 *B* and *D*). Together with the mutational analysis of exon 17 in full-length TRPM3α2 proteins (Fig. 2), these data support the notion that the identified interactions between Gβγ and TRPM3 channels are not only occurring with the short peptide used for obtaining the cocrystal structure but most likely also take place in the full-length proteins in intact cells and are, at least in part, causally responsible for the inhibitory action of Gβγ on TRPM3 channels.

Discussion

Gβγ interacts with a variety of proteins (40), with TRPM3 channels being a very recent addition to the list of Gβγ targets (41). Gβγ binding induces inhibition of TRPM3 channel activity, which has been implicated in reduced nociception (24–26). In this paper, we demonstrate that Gβγ directly binds to TRPM3 and identify an important part of the interaction interface, on both Gβ and TRPM3.

Inhibition of TRPM3 Channels by Gβγ Requires Interacting with Exon 17–Encoded Residues. Our data indicate that TRPM3 inhibition by Gβγ requires binding of Gβγ to TRPM3 on an interaction site, located on the N-terminal cytosolic part of the channel protein. While the dot blot analysis (*SI Appendix*, Fig. S4) seemed to suggest two potential interaction sites on the N terminus, only the second of those is likely to be of physiological relevance. The first, more N-terminal binding site is unlikely to play a functional role in intact cells as truncated TRPM3α2 constructs, which are missing the amino acids encoded by the first three exons, were still found to be inhibited by activating cotransfected μORs (*SI Appendix*, Fig. S1). These truncated channel proteins, however, start at position 89 (cysteine C_{89}) of TRPM3α2 and therefore lack almost the entire first putative Gβγ binding site (which lies in the range of amino acids 81 to 89 of full-length TRPM3α2), which is expected to reduce binding of Gβγ by at least 60% (*SI Appendix*, Fig. S4 *A* and *B*). Furthermore, the position of this site close to the N-terminal end of TRPM3 is likely positioned too far away from the cytosolic face of the plasma membrane to be within reach of the membrane-bound Gβγ proteins. We arrive at this conjecture by considering the recently described 3D structures of other TRPM channels [TRPM2 (42–44), TRPM4 (45–48), TRPM7 (49), and TRPM8 (50, 51)]. These structures show invariably that their N-terminal parts extend quite deeply away from the cytosolic face of the plasma membrane. However, these structures do not contain or do not resolve the very N-terminal part of the channel protein, with the exception of the 3D structure from the zebrafish homolog of TRPM2 (42), which does not have any homology to the N terminus of TRPM3 channels. Therefore, in order to be able to make a more definitive statement, a 3D structure of full-length TRPM3 (which is not yet available) will be needed to confirm the precise position of the N terminus of TRPM3 with respect to the plasma membrane.

The second binding site, on the other hand, as indicated by the dot blot analysis, overlaps with amino acids encoded by exon 17 and is clearly dependent on the presence of specific amino acids (such as K_{595}, which is the second amino acid encoded by exon 17). Also, the likely position of exon 17–encoded amino acids in the full-length protein (as judged from the homologous parts of other TRPM channels for which a 3D structure is available; *SI Appendix*, Fig. S8*C*) is compatible with its proposed role as Gβγ-interacting site. This hypothesis is supported by our analysis of naturally occurring splice variants (Fig. 1), binding studies (*SI Appendix*, Figs. S3–S5), and, importantly, the 3D cocrystal structure of exon 17–encoded peptide bound to Gβγ (Fig. 3). The mutational analysis of TRPM3 exon 17 (Fig. 2 and *SI Appendix*, Fig. S6) and Gβ (Fig. 4 and *SI Appendix*, Fig. S7) provided evidence that the molecular interactions identified in the crystal structure are of functional relevance and are therefore most likely preserved in the full-length proteins under physiological conditions. Removal of exon 17–encoded amino acids did not reduce Gβγ binding to TRPM3 to background values completely (*SI Appendix*, Fig. S5), but we note that coimmunoprecipitation experiments may also report weak and functionally irrelevant binding. The functional analysis of TRPM3α4 and TRPM3α5 splice variants, both lacking exon 17–encoded amino acids, unambiguously demonstrated that these splice variants are not inhibited by increased free Gβγ levels (Fig. 1). These findings were confirmed by studying artificial TRPM3 constructs (lacking N-terminally the amino acids encoded by exons 1 to 3, and all amino acids downstream of P_{1330}; *SI Appendix*, Fig. S1). Also in these constructs, Gβγ-mediated inhibition depended on the presence of the exon 17–encoded amino acids. Our work does not rule out the existence of further, possibly weaker Gβγ binding sites on TRPM3, but our data demonstrate that there is a Gβγ binding site on TRPM3 formed by exon 17–encoded amino acids that is both specific and functionally relevant. A cartoon depicting the spatial relationship between Gβγ and a TRPM channel (TRPM7 as the closest homolog to TRPM3 for which a 3D structure is available) on the cytosolic face of the plasma membrane is given in Fig. 4*E*.

The Exon Encoding the Amino Acids Involved in Gβγ Binding Is Highly Conserved in All Vertebrates. Comparing the TRPM3 sequences from the genomes of a wide and diverse variety of vertebrate species identified the fully conserved sequence encoded by the mouse and human exon 17 (PKALKLLGME) in all these species, even in those that belong to groups that departed very early on from the evolutionary line leading to mammals, such as the sea lamprey *Petromyzon marinus* and the coelacanth *Latimeria chalumnae* (*SI Appendix*, Fig. S8*A*). In the whale shark (*Rhincodon typus*), we found a mutation in the alanine of PKALKLLGME, to valine, and we have included this sequence for this reason in the alignment. This high evolutionary stability (which is seen to a similar extent in the sequences of the preceding exon 16) might indicate that these 10 amino acids serve highly important functions. It will be very interesting to test with functional methods whether TRPM3 channels from these animals are also regulated by Gβγ subunits and therefore by GPCR signaling events.

Alternative Splicing at Exon 17 Is an On–Off Switch for the Inhibitory Control of TRPM3 Channels by Gβγ Proteins. TRPM3 proteins are subject to alternative splicing at at least four different sites in the N terminus alone, and this includes the alternative splicing of exon 17. Additionally, alternative splicing occurs in the C terminus and in the pore region (11, 32, 33). The analysis of several splice variants shows that the splice event at exon 17 is an on–off switch for the ability of TRPM3 channels to be inhibited by Gβγ, and thus to be regulated by GPCR activation (Fig. 1). Comparing the different splice variants, it becomes clear that the splice event at exon 17 operates independently of the splice events at exon 8 or exon 15. Using a human TRPM3 construct [containing exon 2–encoded but lacking exon 1–encoded amino acids (10, 34)] and an artificially shortened TRPM3 construct (lacking amino acids of the three most N-terminal exons, and a substantial amount of amino acids in the C terminus; *SI Appendix*, Fig. S1), we arrived at the conclusion that Gβγ-mediated inhibition of TRPM3 is also independent of the alternative exon usage at the N terminus or the splice event in the C terminus. Thus, the splice event at exon 17 is the only splice event regulating

Gβγ-mediated channel inhibition and operates independently of the other splice events. This self-contained module therefore defines, by its presence or absence, the ability of TRPM3 channels to be regulated by GPCR signaling in a Gβγ-dependent manner. An expression analysis in the choroid plexus showed that ∼30% of TRPM3 transcripts lack exon 17 (33), indicating that in this tissue quite a number of Gβγ-insensitive TRPM3 channels might be expected. For other tissues, such information is lacking, as is any knowledge about how the splice event at exon 17 (or any other splice event) of TRPM3 is regulated. These questions might be fruitful areas for future research.

Additionally, it is noteworthy that other channel proteins inhibited by Gβγ proteins, notably N-type voltage-gated Ca^{2+} channels (Cav2.2), are also subject to alternative splicing that alters the efficacy of Gβγ-induced modulation (52–54). This alternative splicing of Cav2.2 therefore affects how GPCR, and in particular μOR, signaling is capable of modulating transmission of nociceptive signals at the synapse between nociceptors and first-order spinal interneurons. Ultimately, alternative splicing of Cav2.2 channels influences the effectiveness of opioid analgesia (52–54). The effect of alternative splicing that we report here for the TRPM3–Gβγ interaction appears more pronounced than what has been described for Cav2.2 channels, because Gβγ-mediated inhibition of TRPM3 is literally turned on or off depending on the presence or absence of exon 17–encoded amino acids. Alternative splicing of exon 17 therefore constitutes a binary on–off switch for Gβγ-mediated inhibition.

Structural Implications of Gβγ Binding to TRPM3 Channels. It has long been recognized that the cytosolic N terminus of TRPM channels is structured by four regions of relatively high homology (therefore termed TRPM homology regions, MHR1–4) shared by all eight members of this subfamily (55, 56). The amino acids encoded by TRPM3 exon 17 are located between MHR3 and MHR4, and do not share any homology to other TRPM channels, with the exception of TRPM1 (the TRPM protein most closely related to TRPM3; *SI Appendix*, Fig. S8*B*), in which these amino acids are fully conserved (but not known to be subject to alternative splicing). Of note, TRPM1 channels have also been reported to be inhibited by Gβγ subunits, and Gβγ subunits bind these channel proteins preferentially on the N terminus (57, 58).

The linker region between MHR3 and MHR4 is only partially defined in the available cryo-electron microscopy structures of TRPM channels (42, 44–50), with the notable exception of recent structures for TRPM2 (43). Importantly, however, all of these structures, even those that do not fully resolve the relevant amino acid residues of the MHR3–4 linker, indicate that this linker region is located at the outer surface of the protein and therefore easily accessible to protein–protein interactions. Its distance from the cytosolic face of the plasma membrane is highly compatible with binding to the (membrane-bound) Gβγ dimer (*SI Appendix*, Fig. S8*C*).

Our data indicate that the exon 17–encoded peptide assumes an α-helical structure only when bound to Gβγ but folds as random coil when in solution (Fig. 3*C*). It is an appealing thought that the exon 17–encoded region behaves similarly when part of the full-length channel. However, our data are insufficient to make a firm statement about the secondary structure of this part of the protein when not bound by Gβγ, as it is entirely possible that the surrounding parts of the full-length TRPM3 channel influence the secondary structure adopted by the exon 17–encoded residues in the absence of Gβγ binding. Interestingly, the MHR3–4 linker of TRPM2 appears rather unstructured in some 3D reconstructions (43), while this region in TRPM7 proteins has been reported (49) to adopt, at least in part, an α-helical conformation (*SI Appendix*, Fig. S8*C*).

Comparison of TRPM3 Exon 17 and SIGK Peptide during Binding to Gβγ. The TRPM3 exon 17–encoded peptide shows weak (50%) overall sequence homology to a peptide termed "SIGK" (39) that was discovered via phage display to bind Gβγ (*SI Appendix*, Fig. S9*A*). Interestingly, however, the amino acid residues that are highly important for the interaction of Gβγ proteins with exon 17–encoded amino acids of TRPM3 are conserved between the SIGK peptide and exon 17 of TRPM3. The SIGK peptide was also cocrystallized with Gβγ (39) and the built parts of the structures reported by Davis et al. (39) and in this paper are highly similar (rmsd of 0.42 Å). Importantly, the peptides show the same overall binding conformation (*SI Appendix*, Fig. S9*B*). The direct polar contacts are conserved in both of the structures, except for the one formed with the N-terminal primary amino group from the TRPM3 peptide. Indeed, three of the four exon 17–encoded residues of the TRPM3 peptide that provide important interactions with Gβ are also conserved in SIGK: K_{595}, $A_{596,}$ and L_{600} of TRPM3. L_{599} of TRPM3 is an isoleucine in SIGK and therefore very similar. Additionally, G_{601} is conserved, which is not directly undergoing interactions. However, the glycine may be necessary for the observed backbone conformation, since another amino acid may not allow enough flexibility for the sharp kink at this position and the side chain would be in steric hindrance with the bulky W332 side chain of $Gβ_1$. K_{598} is also conserved, but this may be coincidental, as in other Gβγ-binding peptides identified in phage displays and homologous to SIGK (39, 59) this lysine residue is not conserved. Considering the similarities in binding, it is not surprising that the mutational analysis of $Gβ_1$ proteins yields very similar results when comparing binding of SIGK (39) to the inhibition of TRPM3 channels (this work). Of the amino acids tested in both screens (figure 4 of ref. 39 and Fig. 4 of this paper), only $Gβ_1$ D186A yielded differing results. This, however, can easily be explained by the fact that D186 only interacts with the N-terminal serine of SIGK peptide, which would lie outside of the exon 17–encoded region and is not found in TRPM3. Essentially, therefore, the phage display experiments by Davis et al. (39) led to the discovery of a novel peptide (the SIGK peptide), which utilizes the same interface and conformation when binding to Gβγ as nature has evolved for the exon 17–encoded residues of TRPM3. Of note, it has been reported that gallein, a small molecule discovered for its ability to inhibit association of the SIGK peptide with Gβγ, reduces TRPM3 channel inhibition by GPCR activation (25).

The Binding Interface on Gβ Proteins for Interaction with TRPM3. No consensus motif has been identified for the interaction of Gβγ proteins with their various target proteins, and it has been argued that Gβ proteins can adopt a variety of conformations that support different recognition modes for different targets (60). The binding site in Gβγ for the peptide is a site that is utilized to interact with several other proteins as well. For instance, Gα in the heterotrimeric G-protein complex binds to this site via an α-helix, which has no apparent homology to the TRPM3 peptide, and forms additional interactions with the outer wall of the β-propeller (37). Therefore, in a cellular context, Gβγ needs to dissociate at least somewhat from activated Gα in order to bind to TRPM3. An overview of the binding interfaces observed in solved structures of Gβγ in complex with one of its targets is given in *SI Appendix*, Fig. S10 and shows that the binding sites for several different targets strongly overlap with the binding area for the TRPM3 exon 17–encoded peptide at the Gβγ surface (yellow area in *SI Appendix*, Fig. S10). This area has been previously identified as an interaction hot spot (60), meaning that it accommodates the interaction with a large variety of interaction partners. Despite the overlapping interaction interfaces, however, each individual binding partner seems to interact by using a unique combination of amino acid residues for the molecular binding. The uniqueness of the TRPM3–Gβγ binding interface therefore may allow for specifically

designed small molecules (60, 61) to act at this interface and to modulate the TRPM3–Gβγ interaction with some specificity, thereby altering TRPM3 function without strong off-target effects. The findings reported here set the stage for future work to capitalize on this newly described interface and the interaction possibilities it offers. Selective, drug-mediated enhancement of the Gβγ-TRPM3 interaction, for example, could prove to be useful as a novel analgesic principle or as a pharmacotherapy against inflammatory conditions.

Materials and Methods

The following methods were performed using previously published or standard procedures. Brief accounts of methodological details are given in *SI Appendix, Supplementary Materials and Methods*: expression and purification of TRPM3 exon 17–encoded peptide fused to His-tagged maltose-binding protein; dot blot analysis; construction of cDNA clones for N-terminally yellow fluorescent protein (YFP)-tagged mouse TRPM3α5 (YFP-TRPM3α5), truncated TRPM3α2 and TRPM3α5 (as used in *SI Appendix*, Fig. S1 *B* and *C*) and mutants of murine TRPM3α2 and human $Gβ_1$; generation of a HEK293 cell line stably expressing murine YFP-TRPM3α5; culture, handling, and transient transfection of HEK293 cells and HEK293 cells, which stably express either mouse Myc-TRPM3α2-eYFP (11) or mouse YFP-TRPM3α5 (discussed above); Ca^{2+} imaging and whole-cell patch-clamp electrophysiology; electrophysiology of *X. laevis* oocytes; coimmunoprecipitation experiments; Western blotting; cocrystallization of $Gβ_1γ_2$(C68S) with a peptide encoded by TRPM3 exon 17; X-ray data collection, structure building, and refinement; Ni^{2+} column pull-down binding experiments; BLI binding experiments; circular dichroism spectroscopy; and expression and purification of $Gβ_1γ_2$(C68S). In addition, we used a further, different sample of purified $Gβ_1γ_2$ which carried a His-tag and was only used for the dot blot analysis. This second sample of purified $Gβ_1γ_2$ was a kind gift of Jochen Schwenk, University of Freiburg, Freiburg, Germany. It was prepared exactly as described previously (62).

Statistics. Descriptive statistics and statistical testing were performed using established standards. The full details are given in *SI Appendix, Supplementary Materials and Methods*.

Data Availability. The coordinates and structure factors of the crystal structure have been deposited in the Protein Data Bank (PDB) under accession code 6RMV. The accession numbers of the previously published (11, 33) TRPM3 splice variants are: TRPM3α2: NP_001030319; TRPM3α3: NP_001030317; TRPM3α4: NP_001030318; TRPM3α5: NP_001030320; and TRPM3α6: XP_006527024.

ACKNOWLEDGMENTS. We thank Dr. Jochen Schwenk (Freiburg, Germany) for his kind gift of His-tagged Gβγ proteins and Drs. Moritz Bünemann (Marburg, Germany), Mike Zhu (Dallas, TX), and Tooraj Mirshahi (Geisinger Clinic, Danville, PA) for clones. The authors are grateful to Dr. Annie Beuve (Rutgers New Jersey Medical School) for allowing us to use her fluorescence microscope. We thank beamline staff at ID30B of the European Synchrotron Radiation Facility (Grenoble). The Switch Laboratory was supported by grants from the European Research Council (ERC) under European Union Horizon 2020 Framework Program ERC grant agreement 647458 (MANGO) to J.S., the Flanders Institute for Biotechnology (VIB; grant C0401), the Industrial Research Fund of KU Leuven ("Industrieel Onderzoeksfonds"), the Funds for Scientific Research Flanders (FWO; Hercules Foundation grant AKUL/15/34 – G0H1716N), and the Flanders Agency for Innovation by Science and Technology (IWT; SBO grant 60839). The laboratory of A.E. was supported by grants from KU Leuven (MeNaGe: #RUN/16/001, FOscil: ZKD4582 - C16/18/008, ProFlow: FWO/F.R.S.-FNRS "Excellence of Science" #30550343) and FWO (CARBS: #G0C6814N). N.L. was funded by Fund for Scientific Research Flanders Postdoctoral Fellowship (FWO 12P0919N), as was V.Z. (FWO 12W4618N). This work was further supported by NIH grants R01 NS055159 and R01 GM093290 to T.R., a HOMFOR grant from Universität Saarbrücken to S.E.P., the FWO-Vlaanderen research project G0C9717N and KU Leuven C14/17/093 to C.U., and the DFG program SFB 593 to J.O. F.G. is supported by European Union's Horizon 2020 research and innovation program under Marie Skłodowska-Curie Grant 665501 with the research Foundation Flanders (FWO-Vlaanderen). F.G. is a FWO [PEGASUS]^2 Marie Skłodowska-Curie Fellow.

1. A. I. Basbaum, D. M. Bautista, G. Scherrer, D. Julius, Cellular and molecular mechanisms of pain. *Cell* **139**, 267–284 (2009).
2. D. Julius, TRP channels and pain. *Annu. Rev. Cell Dev. Biol.* **29**, 355–384 (2013).
3. J. E. Sexton, J. Vernon, J. N. Wood, TRPs and pain. *Handb. Exp. Pharmacol.* **223**, 873–897 (2014).
4. J. Vriens *et al*., TRPM3 is a nociceptor channel involved in the detection of noxious heat. *Neuron* **70**, 482–494 (2011).
5. I. Vandewauw *et al*., A TRP channel trio mediates acute noxious heat sensing. *Nature* **555**, 662–666 (2018).
6. O. Alkhatib *et al*., Promiscuous G-protein-coupled receptor inhibition of Transient Receptor Potential Melastatin 3 ion channels by Gβγ subunits. *J. Neurosci.* **39**, 7840–7852 (2019).
7. M. L. Nealen, M. S. Gold, P. D. Thut, M. J. Caterina, TRPM8 mRNA is expressed in a subset of cold-responsive trigeminal neurons from rat. *J. Neurophysiol.* **90**, 515–520 (2003).
8. S. G. Lechner, H. Frenzel, R. Wang, G. R. Lewin, Developmental waves of mechanosensitivity acquisition in sensory neuron subtypes during embryonic development. *EMBO J.* **28**, 1479–1491 (2009).
9. I. Vandewauw, G. Owsianik, T. Voets, Systematic and quantitative mRNA expression analysis of TRP channel genes at the single trigeminal and dorsal root ganglion level in mouse. *BMC Neurosci.* **14**, 21 (2013).
10. C. Grimm, R. Kraft, S. Sauerbruch, G. Schultz, C. Harteneck, Molecular and functional characterization of the melastatin-related cation channel TRPM3. *J. Biol. Chem.* **278**, 21493–21501 (2003).
11. J. Oberwinkler, A. Lis, K. M. Giehl, V. Flockerzi, S. E. Philipp, Alternative splicing switches the divalent cation selectivity of TRPM3 channels. *J. Biol. Chem.* **280**, 22540–22548 (2005).
12. T. F. J. Wagner *et al*., Transient receptor potential M3 channels are ionotropic steroid receptors in pancreatic β cells. *Nat. Cell Biol.* **10**, 1421–1430 (2008).
13. T. F. J. Wagner *et al*., TRPM3 channels provide a regulated influx pathway for zinc in pancreatic beta cells. *Pflugers Arch.* **460**, 755–765 (2010).
14. Y. Majeed *et al*., Pregnenolone sulphate-independent inhibition of TRPM3 channels by progesterone. *Cell Calcium* **51**, 1–11 (2012).
15. A. Drews *et al*., Structural requirements of steroidal agonists of transient receptor potential melastatin 3 (TRPM3) cation channels. *Br. J. Pharmacol.* **171**, 1019–1032 (2014).
16. L. Demirkhanyan, K. Uchida, M. Tominaga, E. Zakharian, TRPM3 gating in planar lipid bilayers defines peculiar agonist specificity. *Channels (Austin)* **10**, 258–260 (2016).
17. P. Geppetti, N. A. Veldhuis, T. Lieu, N. W. Bunnett, G protein-coupled receptors: Dynamic machines for signaling pain and itch. *Neuron* **88**, 635–649 (2015).
18. N. A. Veldhuis, D. P. Poole, M. Grace, P. McIntyre, N. W. Bunnett, The G protein-coupled receptor-transient receptor potential channel axis: Molecular insights for targeting disorders of sensation and inflammation. *Pharmacol. Rev.* **67**, 36–73 (2015).
19. Y. Yudin, T. Rohacs, Inhibitory $G_{i/O}$-coupled receptors in somatosensory neurons: Potential therapeutic targets for novel analgesics. *Mol. Pain* **14**, 1744806918763646 (2018).
20. C. Stein, Opioids, sensory systems and chronic pain. *Eur. J. Pharmacol.* **716**, 179–187 (2013).
21. C. Stein *et al*., Peripheral mechanisms of pain and analgesia. *Brain Res. Brain Res. Rev.* **60**, 90–113 (2009).
22. G. W. Pasternak, Y.-X. Pan, Mu opioids and their receptors: Evolution of a concept. *Pharmacol. Rev.* **65**, 1257–1317 (2013).
23. C. Stein, Opioid receptors. *Annu. Rev. Med.* **67**, 433–451 (2016).
24. D. Badheka *et al*., Inhibition of transient receptor potential melastatin 3 ion channels by G-protein βγ subunits. *eLife* **6**, e26147 (2017).
25. T. Quallo, O. Alkhatib, C. Gentry, D. A. Andersson, S. Bevan, G protein βγ subunits inhibit TRPM3 ion channels in sensory neurons. *eLife* **6**, e26138 (2017).
26. S. Dembla *et al*., Anti-nociceptive action of peripheral mu-opioid receptors by G-beta-gamma protein-mediated inhibition of TRPM3 channels. *eLife* **6**, e26280 (2017).
27. K. K. Touhara, R. MacKinnon, Molecular basis of signaling specificity between GIRK channels and GPCRs. *eLife* **7**, e42908 (2018).
28. I. Masuho *et al*., Molecular deconvolution platform to establish disease mechanisms by surveying GPCR signaling. *Cell Rep.* **24**, 557–568.e5 (2018).
29. N. Volkow, H. Benveniste, A. T. McLellan, Use and misuse of opioids in chronic pain. *Annu. Rev. Med.* **69**, 451–465 (2018).
30. C. E. Ford *et al*., Molecular basis for interactions of G protein βγ subunits with effectors. *Science* **280**, 1271–1274 (1998).
31. M. R. Whorton, R. MacKinnon, X-ray structure of the mammalian GIRK2-βγ G-protein complex. *Nature* **498**, 190–197 (2013).
32. N. Lee *et al*., Expression and characterization of human transient receptor potential melastatin 3 (hTRPM3). *J. Biol. Chem.* **278**, 20890–20897 (2003).
33. J. Frühwald *et al*., Alternative splicing of a protein domain indispensable for function of transient receptor potential melastatin 3 (TRPM3) ion channels. *J. Biol. Chem.* **287**, 36663–36672 (2012).
34. J. Oberwinkler, S. E. Philipp, TRPM3. *Handb. Exp. Pharmacol.* **222**, 427–459 (2014).
35. J. A. Iñiguez-Lluhi, M. I. Simon, J. D. Robishaw, A. G. Gilman, G protein βγ subunits synthesized in Sf9 cells. Functional characterization and the significance of prenylation of γ. *J. Biol. Chem.* **267**, 23409–23417 (1992).
36. J. Przibilla *et al*., Ca^{2+}-dependent regulation and binding of calmodulin to multiple sites of transient receptor potential melastatin 3 (TRPM3) ion channels. *Cell Calcium* **73**, 40–52 (2018).
37. M. A. Wall *et al*., The structure of the G protein heterotrimer $G_{iα1}β_1γ_2$. *Cell* **83**, 1047–1058 (1995).
38. J. Sondek, A. Bohm, D. G. Lambright, H. E. Hamm, P. B. Sigler, Crystal structure of a G_A protein βγ dimer at 2.1Å resolution. *Nature* **379**, 369–374 (1996).

39. T. L. Davis, T. M. Bonacci, S. R. Sprang, A. V. Smrcka, Structural and molecular characterization of a preferred protein interaction surface on G protein βγ subunits. *Biochemistry* **44**, 10593–10604 (2005).
40. S. M. Khan *et al*., The expanding roles of Gβγ subunits in G protein-coupled receptor signaling and drug action. *Pharmacol. Rev.* **65**, 545–577 (2013).
41. A. V. Smrcka, I. Fisher, G-protein βγ subunits as multi-functional scaffolds and transducers in G-protein-coupled receptor signaling. *Cell. Mol. Life Sci.* **76**, 4447–4459 (2019).
42. Y. Huang, P. A. Winkler, W. Sun, W. Lü, J. Du, Architecture of the TRPM2 channel and its activation mechanism by ADP-ribose and calcium. *Nature* **562**, 145–149 (2018).
43. L. Wang *et al*., Structures and gating mechanism of human TRPM2. *Science* **362**, eaav4809 (2018).
44. Z. Zhang, B. Tóth, A. Szollosi, J. Chen, L. Csanády, Structure of a TRPM2 channel in complex with Ca^{2+} explains unique gating regulation. *eLife* **7**, e36409 (2018).
45. J. Guo *et al*., Structures of the calcium-activated, non-selective cation channel TRPM4. *Nature* **552**, 205–209 (2017).
46. P. A. Winkler, Y. Huang, W. Sun, J. Du, W. Lü, Electron cryo-microscopy structure of a human TRPM4 channel. *Nature* **552**, 200–204 (2017).
47. H. E. Autzen *et al*., Structure of the human TRPM4 ion channel in a lipid nanodisc. *Science* **359**, 228–232 (2018).
48. J. Duan *et al*., Structure of full-length human TRPM4. *Proc. Natl. Acad. Sci. U.S.A.* **115**, 2377–2382 (2018).
49. J. Duan *et al*., Structure of the mammalian TRPM7, a magnesium channel required during embryonic development. *Proc. Natl. Acad. Sci. U.S.A.* **115**, E8201–E8210 (2018).
50. Y. Yin *et al*., Structure of the cold- and menthol-sensing ion channel TRPM8. *Science* **359**, 237–241 (2018).
51. M. M. Diver, Y. Cheng, D. Julius, Structural insights into TRPM8 inhibition and desensitization. *Science* **365**, 1434–1440 (2019).
52. A. Andrade, S. Denome, Y.-Q. Jiang, S. Marangoudakis, D. Lipscombe, Opioid inhibition of N-type Ca^{2+} channels and spinal analgesia couple to alternative splicing. *Nat. Neurosci.* **13**, 1249–1256 (2010).
53. Y.-Q. Jiang, A. Andrade, D. Lipscombe, Spinal morphine but not ziconotide or gabapentin analgesia is affected by alternative splicing of voltage-gated calcium channel $Ca_V2.2$ pre-mRNA. *Mol. Pain* **9**, 67 (2013).
54. D. Lipscombe, A. Andrade, S. E. Allen, Alternative splicing: Functional diversity among voltage-gated calcium channels and behavioral consequences. *Biochim. Biophys. Acta* **1828**, 1522–1529 (2013).
55. D. E. Clapham, TRP channels as cellular sensors. *Nature* **426**, 517–524 (2003).
56. A. Fleig, R. Penner, The TRPM ion channel subfamily: Molecular, biophysical and functional features. *Trends Pharmacol. Sci.* **25**, 633–639 (2004).
57. Y. Shen, M. A. F. Rampino, R. C. Carroll, S. Nawy, G-protein-mediated inhibition of the Trp channel TRPM1 requires the Gβγ dimer. *Proc. Natl. Acad. Sci. U.S.A.* **109**, 8752–8757 (2012).
58. Y. Xu *et al*., The TRPM1 channel in ON-bipolar cells is gated by both the α and the βγ subunits of the G-protein G_o. *Sci. Rep.* **6**, 20940 (2016).
59. J. K. Scott *et al*., Evidence that a protein-protein interaction 'hot spot' on heterotrimeric G protein βγ subunits is used for recognition of a subclass of effectors. *EMBO J.* **20**, 767–776 (2001).
60. Y. Lin, A. V. Smrcka, Understanding molecular recognition by G protein βγ subunits on the path to pharmacological targeting. *Mol. Pharmacol.* **80**, 551–557 (2011).
61. A. P. Campbell, A. V. Smrcka, Targeting G protein-coupled receptor signalling by blocking G proteins. *Nat. Rev. Drug Discov.* **17**, 789–803 (2018).
62. R. Turecek *et al*., Auxiliary $GABA_B$ receptor subunits uncouple G protein βγ subunits from effector channels to induce desensitization. *Neuron* **82**, 1032–1044 (2014).